Enhancing MPPT in Partially Shaded PV Modules: A Novel Approach using Adaptive Reinforcement Learning with Neural Network Architecture

M. Leelavathi[1*], and V. Suresh Kumar[2]

[1,2]Thiagarajar College of Engineering, Madurai, Tamil Nadu, India

Abstract. The occurrence of partial shading in solar power systems presents a substantial challenge with widespread implications, sparking extensive research, notably in the field of Maximum Power Point Tracking (MPPT).This study emphasizes the critical process of accurately tracking the maximum power points with the characteristic curves of Photovoltaic (PV) modules under real-time, diverse partial shading patterns. It explores the various stages of the tracking process and the methodologies employed for optimization. While conventional methods have shown effectiveness, they often fall short in swiftly and accurately tracking maximum power points with minimal errors. To address this limitation, this research introduces a novel machine learning approach known as Adaptive Reinforcement Learning with Neural Network Architecture (ARL-NNA) for MPPT. The results obtained from ARL-NNA are compared with existing algorithms using the same experimental data. Furthermore, the outcomes are validated through different factors and processing time measurements. The findings conclusively demonstrate the efficacy and superiority of the proposed algorithm in effectively tracking maximum power points in PV characteristic curves, providing a promising solution for optimizing solar energy generation in partial shading patterns. This study significantly impacts various realms of electrical engineering including power engineering, power electronics, industrial electronics, solid state electronics, energy technology and other related field of Engineering and Technology.

Keywords: Machine learning; Maximum power point tracking; Partial shading patterns; Photovoltaic module; Renewable energy

1. INTRODUCTION

The diminishing reserves of conventional energy sources used for electricity generation are closely linked to the deterioration of our natural resource ecosystem. Consequently, solar energy systems have long been regarded as a dependable means of satisfying both energy demand and efficiency requirements. According to International Energy Agency (IEA) [1], the global solar energy generation has accelerated by 270 terawatts in 2022 aligning with the estimated Net Zero Emissions target of 2030. However, the widespread adoption of solar energy systems faces challenges in many regions due to factors such as cloud cover, snowfall, continuous rainfall, localized hotspots, obstructions from buildings, interference from birds, and waste accumulation. Despite its integration into various sectors, including engineering applications, residential use, industrial applications, commercial enterprises, and even water desalination; solar energy systems come with several limitations.

Figure 1 illustrates the leading nations in solar installation worldwide and highlights how their presence contributes to conditions of partial shading [2-5].
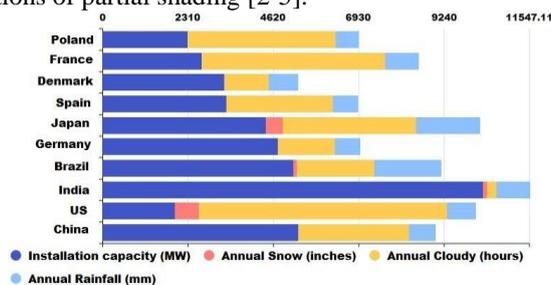

Fig.1. Survey of solar installation and affected range

Likewise, it can be seen from Fig.1 that Faroe Island, Denmark,

experiences a particularly challenging cloudy conditions, with an average of only 2.4 hours of sunshine per day and a mere 840 hours of annual sunshine [6]. Moving to the state of Meghalaya in India, both Mawsynram and Cherrapunji are noteworthy for their exceptionally high annual rainfall, which averages at a staggering 11,871 millimeters [7]. In the mountainous regions of north-western Japan, a long-standing climatic feature is the annual snowfall, which can accumulate to a remarkable depth of up to 125 feet [8, 9].

Harnessing energy from natural light sources using photovoltaic (PV) modules stands as the most prevalent means of electricity generation. In this process, light energy undergoes conversion into electrical energy. PV modules primarily rely on fundamental parameters like solar illumination and temperature. However, the emergence of global warming and the ever-fluctuating and unstable meteorological conditions have led to frequent variations in these basic parameters. Consequently, the performance of PV modules is susceptible to inaccuracies in power generation. Moreover, inconsistent power output can disrupt the continuous supply of electricity to the energy load. Therefore, it becomes crucial to analyze PV module performance under various partial shading scenarios. Before delving into the analysis of partial shading effects, it is essential to extract unknown electrical parameters of PV modules. These parameters are typically determined through an optimization process or in analytical methods, even in the face of changing meteorological conditions [10].

In addition to the unknown electrical parameters, various partial shading patterns significantly impact the performance of PV modules. Partial shading can occur due to diverse factors, including the movement of cloud patterns, shading from trees, buildings, and adjacent PV modules, the presence of bird droppings, dust particles, damaged or broken PV cells, snowfall, and rain. Moreover, some research endeavors specifically explore the array of partial shading patterns

*e-mail: leelavathi@student.tce.edu

www.czasopisma.pan.pl   PAN   www.journals.pan.pl

Enhancing MPPT in Partially Shaded PV Modules: A Novel Approach using Adaptive Reinforcement Learning with Neural Network Architecture

occurring under different weather conditions. Sudden shifts in meteorological conditions can also lead to fluctuations in the unknown electrical parameters, consequently affecting the output values of PV modules [11].

These fluctuations in output values can have repercussions, potentially causing variations in the performance of electrical appliances connected to the PV modules or even causing damage. To ensure that the maximum output values of PV modules are consistently achieved, the Maximum Power Point Tracking (MPPT) [12-15] technique, based on optimization processes, is employed. This technique remains effective even in the face of changing meteorological conditions or partial shading patterns. The output values of PV modules exhibit significant changes, with characteristic curves featuring both global maximum and local minimum peak points. The MPPT optimization process can be categorized into three distinct groups: classical algorithms [16, 17], bio-inspired algorithms [18-24], and soft computing algorithms [25-30].

Classical MPPT [16,17] algorithms like Perturb and Observe (P&O), Incremental Conductance (InC), Constant Voltage (CV), and Hill-Climbing (HC) and coexist with bio-inspired [18-24] counterparts such as Particle Swarm Optimization (PSO), Genetic Algorithm (GA), Flower Pollination (FP), Artificial Bee Colony (ABC), and Cuckoo Search (CS). These algorithms are designed to identify optimal points on characteristic curves but often face challenges such as oscillations and fluctuating results. Additionally, soft computing techniques [25-30] like Fuzzy Logic Control (FLC), Artificial Neural Networks (ANN), Deep Learning (DL), and Machine Learning (ML) contribute to MPPT capabilities, although they may exacerbate oscillation issues. Recently, Reinforcement Learning (RL) has emerged as a promising approach in the optimization processes of the Machine Learning (ML) domain, specifically excelling in tasks such as global maximum point tracking, albeit with essential considerations of stability and consistency. The choice of technique depends on specific application contexts and requirements.

In summary, the previous research work has highlighted the significance of identifying the maximum peak point in PV modules subjected to various partial shading patterns and by using various optimization techniques including machine learning method. Due to various partial shading patterns, the parameters like voltage, current, and power values of the PV module significantly change. Likewise, the interconnected real-time application like grid, residential, commercial and industrial connections lead to a mismatching loss. Through this mismatching loss surrounds a huge power loss. In PV modules, the impact of partial shading conditions often poses a challenge, and conventional MPPT algorithms frequently prove insufficient in precisely tracking the maximum power point. This is particularly evident in situations characterized by partial shading or fluctuating conditions. Most of the existing algorithms reliant on iterative methods and hence struggle to swiftly identify new global maximum points, leading to inconsistent readings. Moreover, existing soft computing algorithms for MPPT in partially shaded settings can be computationally intensive.

To address these challenges, this work proposes an innovative approach that combines Reinforcement Learning (RL) with Neural Network Architecture (NNA) algorithm from Machine Learning. This novel idea leverages RL's state, action, and reward parameters along with the capabilities of NNA. The method holds promise for achieving more precise and efficient Maximum Power Point Tracking (MPPT). It can adapt quickly to changing conditions and has the potential to deliver superior results in the quest for tracking the maximum power point.

Moreover, this research introduces a novel approach involving dual Neural Network Architecture (NNA) to enhance data training and optimization. In this approach, NNA is dedicated to collecting data points that closely align with the actual input, ensuring greater accuracy in the learning process and also the NNA plays a vital role by identifying and filtering out residual values that significantly deviate from the actual input, thereby reducing the storage burden, especially within the action parameter. The culmination of this innovative approach lies in the careful design and optimization of the reward function. This component holds a pivotal role in reinforcement learning algorithms, and in this study, it has been customized to select the most appropriate reward values, ultimately shaping the outcome of the MPPT process.

In summary, this pioneering methodology not only fills a crucial research gap but also provides a novel solution for the management and control of photovoltaic modules. The integration of the Adaptive Reinforcement Learning-Neural Network Architectures (ARL-NNA) within the Machine Learning (ML) algorithm exhibits significant promise, particularly in addressing the intricate challenges posed by diverse partial shading scenarios. The algorithm presented in this study exhibits versatility across various applications; including text summarization, machine learning, prediction, and optimization control. Its notable capability to facilitate automatic decision-making represents a substantial contribution to the advancement of solar energy systems.

The proposed research work follows a structured approach as outlined below:

i. Parameter Extraction: The characteristic curve values of unknown electrical parameters of PV module are extracted.

ii. ARL-NNA Implementation: The implementation of the proposed ARL-NNA within the Machine Learning (ML) method is performed.

iii. Result and Analysis: Proposed approach is evaluated with existing algorithms to assess its performance, and effectiveness with a thorough discussion of the outcomes in detail.

iv. Validation: Finally, the results are subjected to validation through different factors and processing time, ensuring the robustness and reliability of the proposed method.

2. MATERIALS AND METHODS

In this section, the study introduces a mathematical equation that characterizes the electrical behavior of a PV module. Also, it delineates the methodology for solving the fundamental PV module equation by leveraging experimental data. Initially, the equation for extracting unknown electrical parameters is presented, followed by the derivation of the current equation of the PV module using Newton-Raphson method.

2.1. Mathematical expression of PV module

Here, the objective is to establish the unknown electrical parameter of the PV solar cell output current (I_o). The I_o which is parameterized using Kirchhoff's laws with photo generation current (I_{ph}), diode junction current (I_{di}), and shunt resistance current (I_{sh}), as in equation (1) [31,32]. The circuit diagram

2

www.czasopisma.pan.pl   PAN   www.journals.pan.pl

Enhancing MPPT in Partially Shaded PV Modules: A Novel Approach using Adaptive Reinforcement Learning with Neural Network Architecture

based on single-diode equation for the PV module is depicted in Fig. 2.

$$I_o = I_{ph} - I_{di} - I_{sh} \tag{1}$$
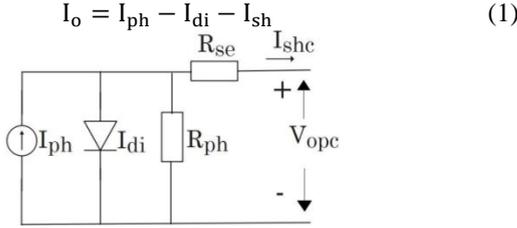
Fig. 2. Equivalent circuit of PV module

In [31], the shunt resistances I_{sh} is discarded because it significantly influence the outcomes of the PV module both in standard testing conditions (STC) and real-world cases. So, equation (2) is retrieved as,

$$I_o = I_{ph} - I_{di} \tag{2}$$

From Shockley's diode junction equation, I_{di} in equation (3) signifies current versus voltage (I-V) characteristics curve equation of a PV solar cell. The I_{ss} represents the reverse saturation current, V_o denotes the load voltage and N_{sr} signifies the number of series connections in the PV module.

$$I_{di} = I_{ss} \left[exp \left(\frac{V_o}{GN_{sr}} \right) - 1 \right] \tag{3}$$

Where, $G = \frac{j}{KAT_c}$

G in diode's thermal voltage is represented as (V), K indicates the continual Boltzmann (1.38 x 10-23 J/K), T_c points cell temperature, A =1 is the identical factor and j denotes the electron charge (1.60 x 10^{-19} C).

According to the Standard Testing Condition (STC) and real-world cases, the parasitic resistances like series resistance R_{se} and parallel resistance R_{pa} are demonstrated in the output current equation. Here, R_{se} is highlighted when a large number of PV systems are placed on the ground surface where R_{pa} is neutral. So, the I_{di} the equation can be rewritten as in equation (4).

$$I_{di} = I_{ss} \left[exp \left(\frac{V_o + I_o R_{se}}{GN_{sr}} \right) - 1 \right] \tag{4}$$

The general PV module output current equation is illustrated in equation (5), with the series-parallel arrangement in the large number of PV module.

$$I_o = N_{pa} * I_{ph} - N_{pa} * I_{ss} \left[exp \left(\frac{V_o + I_o R_{se}}{GN_{sr}} \right) - 1 \right] \tag{5}$$

In this work, a single PV module with 36 cells is associated with the series-parallel relationship. Since the PV module is propagated in a parallel correlation, the value of N_{pa}=1 [31] and equation (5) is personalized accordingly as given in equation (6).

$$I_o = I_{ph} - I_{ss} \left[exp \left(\frac{V_o + I_o R_{se}}{GN_{sr}} \right) - 1 \right] \tag{6}$$

The I_{ph} based on the continuous change of solar illumination G_c in (W/m^2), temperature values T_c in (°C) along with STC (G_{st} in W/m^2 and T_{st} in °C) is symbolized in equation (7).

$$I_{ph} = [I_{sc} + K_i(T_c - T_{st})] * \left(\frac{G_c}{G_{st}} \right) \tag{7}$$

Equations (8 and 9) embody the reverse saturation current I_{res} and saturation current I_{sc}, approximately with stable ideality factor and energy bandgap.

$$I_{res} = I_{ss} / exp \left[\left(\frac{jV_{oa}}{GN_{sr}} \right) - 1 \right] \tag{8}$$

$$I_{sc} = I_{res} \left[\left(\frac{T_c}{T_{st}} \right) \right]^3 exp \left[\left(\frac{jEg}{AK} \right) \left(\frac{1}{T_{st}} \right) - \left(\frac{1}{T_c} \right) \right] \tag{9}$$

2.2. Unknown electrical parameters (UEP) of PV module

The UEP equation [31] encapsulates vital input parameters, including short-circuit current (I_{shc}), open-circuit voltage (V_{opc}),

and maximum voltage, current, and power (V_{maxp}, I_{maxp}, and P_{maxp}). These parameters are computed through equations (10) to (14). Subsequently, the UEP input parameters are utilized in the current equation (I_o) and seamlessly integrated into the analytical Newton-Raphson method. The ensuing UEP equations are then extracted through the corresponding procedural steps.

● Short circuit current I_{shc} is positioned at the load terminal. So, $I_{ph} = I_{shc}$ and $V_o = 0$ are substituted in equation (5), where the I_{shc} is shown in equation (10). Where saturation current I_{so} and shunt resistance R_{ph}.

$$I_{shc} = I_{ph} - I_{ss} \left[(exp(\frac{I_{shc}R_{se}}{G}) - 1) - \frac{I_{so}R_{se}}{R_{ph}} \right] \tag{10}$$

● Open circuit voltage V_{opc} in (V) is direct at the load terminal. So, $I_{shc}=0$ and $V_o=V_{opc}$ are incorporated as presented in equation (11).

$$I_{ph} - I_{ss} \left[exp \left(\frac{V_{opc}}{G} \right) - 1 \right] - \frac{V_{opc}}{R_{ph}} = 0 \tag{11}$$

$$I_{ss} = \frac{I_{ph} - \frac{V_{opc}}{R_{ph}}}{\left(\frac{V_{opc}}{G} \right) - 1} \tag{12}$$

● The maximum current (I_{maxp}), as expressed in equation (13), is established by substituting $V_o=V_{maxp}$ and $I_{ph}=I_{maxp}$ into equation (5). Here, V_{maxp} represents the maximum voltage.

$$I_{maxp} = I_{ph} - I_{ss} \left[exp \left(\frac{V_{maxp} + I_{maxp} * R_{se}}{G} \right) - 1 \right] - \frac{V_{maxp} + I_{maxp} * R_{se}}{R_{ph}} \tag{13}$$

● R_{se}, the series resistance is calculated using equation (14) [32]. Where, diode identity factors (A).

$$R_{se} = \left[\frac{I_{ph} - I_{maxp} - \frac{V_{maxp}}{R_{se}} + I_{ss} \left(1 - e^{\frac{V_{maxp}}{A}} \right)}{I_{maxp} * \frac{I_{ss}}{A} e^{\frac{V_{maxp}}{A}} + \frac{1}{R_{ph}}} \right] \tag{14}$$

Finally, the Newton Raphson method is employed to optimize the output current I_o as represented in equation (15).The parameters like I_o, R_{se}, I_{ph}, A, and R_{ph}, as outlined in Equation 10 - 15, are also essential for extracting values that contribute to accurate system modeling, efficient energy harvesting, and data-driven decision-making, ultimately enhancing the optimal performance and reliability of a PV module.

$$I_o = \left[I_{ph} - \left(\frac{I_{ss} \left[(exp(M) - 1) - I_{ss}(exp(M)) \right]}{-1 - I_{ss} \left[(exp(M) - 1) - I_{ss}(exp(M)) \right]} \right) \right] \tag{15}$$

Where, $M = \frac{V_{maxp} + I_{maxp} R_{se}}{GN_{sr}}$

3. PROPOSED MACHINE LEARNING ALGORITHM

In the current operational background of photovoltaic (PV) modules, the challenges posed by partial shading patterns have prompted the implementation of a crucial solution which is the Maximum Power Point Tracking (MPPT) technique. This research endeavors to elevate the operational efficiency of PV modules by evaluating an advanced novel methodology designed to enhance the MPPT technique. Grounded in keen observations of solar power generation under direct sunlight, this innovative approach aims to address the complexities associated with partial shading patterns. To further process and optimize this methodology, a comprehensive machine learning strategy is employed, combining two distinct approaches. Notably, the research introduces a novel optimization process, Adaptive Reinforcement Learning with Neural Network Architecture (ARL-NNA) algorithm, integrated with the MPPT technique. This global strategy is poised to significantly improve the efficiency and adaptability of PV modules, marking an important advancement in mitigating the challenges posed by partial shading patterns.

3

www.czasopisma.pan.pl   PAN   www.journals.pan.pl

Enhancing MPPT in Partially Shaded PV Modules: A Novel Approach using Adaptive Reinforcement Learning with Neural
Network Architecture

3.1. Classical Reinforcement learning algorithm

The Reinforcement Learning (RL) [25-30], introduced by Bellman in 1957, is a type of machine learning where algorithms learn by striving for the best rewards. This involves two main aspects: firstly, representing a policy as a decision-making strategy, and secondly, adapting and refining strategies over time to improve decision-making abilities. The primary goal is to intelligently navigate and understand the context to achieve the best possible outcomes.

In the RL algorithm, several key parameters, including environment, agent, state, action, and reward, are integral to its operation. The essence of the RL algorithm lies in the agent's interaction with the environment, wherein it receives input values and takes actions that result in rewards or output values. The agent's learning process is based on observing the current situation, known as the state, and aiming to make better decisions in subsequent interactions. The decision-making policy starts by understanding the environment and agent values, and the learning process involves key parameters such as state, action, and reward. This research article introduces a novel approach for tracking the maximum power at characteristic curves, employing adaptive reinforcement learning with neural network architecture, and innovatively incorporating a duty cycle mechanism for increased adaptability and efficiency in Maximum Power Point Tracking (MPPT) under varying environmental conditions.

3.2. Learning process of adaptive RL algorithm

The experimental curves depict the presence of multiple peaks resulting from various partial shading patterns under different weather conditions. The process of identifying the Global Maximum Power Point (GMPP) within the characteristic curve of the PV module using the ARL-NNA algorithm is illustrated in Fig. 3. Because of the changing weather conditions, the Local maximum peak power (LMPP) value is prone to fluctuate. However, with the ARL-NNA algorithm, the Global maximum points can be tracked in a matter of seconds. Consequently, this approach contributes to reducing power losses caused by mismatched conditions.
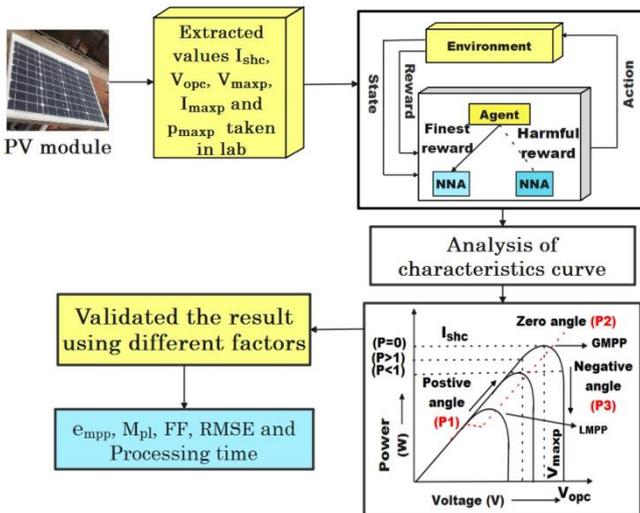

Fig. 3. Overall block diagram

The primary aim of this article is to establish the effectiveness of the ARL-NNA algorithm for effective implementation of MPPT. NNA are chosen due to their ease of testing and training, even with limited data. In this approach, NNA are employed, with each focusing on a specific aspect of the agent function. The NNA is dedicated to segmenting the finest reward, while the other identifies and segments the harmful reward. By doing so, harmful reward values are effectively eliminated, leaving only the finest reward value for the determination of the Global Maximum Power Point Tracking (GMPPT).

Furthermore, the significant contribution of this research work lies in demonstrating that the ARL-NNA algorithm can yield operational results within a fraction of a second. Additionally, it is worth noting that no prior research has explored the testing of the Reinforcement Learning (RL) framework with segmented NNA frame. Moreover, the present study addresses the GMPPT problem within the RL framework by examining it under various learning conditions, as outlined below.

- State: In the specific conditions outlined in [27], the MPPT tracking process involves dealing with unknown electrical input parameters for PV module values, which are managed through an iterative method. Prior to commencing the tracking process, the output of the iterative method is subjected to a new step known as the "duty cycle." This duty cycle plays a critical role in enhancing the tracking process by facilitating the discovery of the (ΔP_{maxp}) maximum power point, which is tracked at zero angles (referred to as P2) on the characteristic curves as shown in Fig. 3. According to equation 16, the state value is characterized by I_{maxp}, V_{maxp}, and ΔP_{maxp}. Consequently, this approach leads to an increase in the maximum power value while reducing error values. The learning stage for the state function, 'S' is defined as follows:

$$S = \{\omega_{j,n}, \Delta P_{maxp_{(j,n)}}, I_{maxp} \in [1,2..j], V_{maxp} \in [1,2..,n]\} \quad (16)$$

In this context, ω stands for weight, while j and n denote the range of the iteration (j,n=1:V_{opc}).

- Action: Through building upon the specification of the state value, the evolution of the ARL-NNA algorithm aims to determine the action value. With the inclusion of the new process, i.e., the duty cycle, an optimized power value ΔP_{maxp} is generated using equation 17.

$$\Delta\omega_{j,n} = \omega_{j,n} + \Delta D(\text{duty cycle}) \quad (17)$$

Equation 18 defines the action set A, where $\Delta\omega_{j,n}$ represents the new weight value, $\Delta D = 0.01$. The values within the set are as follows: $+\omega_{j,n}$ denotes the angle of P1,'0' signifies the angle of P2 and $-\omega_{j,n}$ represents the angle of P3.

$$A = \{+\omega_{j,n}, 0, -\omega_{j,n}\} \quad (18)$$

The negative (P3) value is discarded, and the agent function produces the positive (P1) value for the action function. Subsequently, a loop iterates until the completion of the statement. The agent's role is to reduce the workload associated with locating the maximum search point and passing the results to the action function. This process ensures that the action value operates with higher precision and effective computation.

- Reward: In the process of NNA training for Maximum Power Point Tracking (MPPT), the reward function plays a pivotal role, dynamically responding to environmental conditions and agent values. When the agent function, facilitated by the NNA body, yields a positive (P1) fitness reward, the reward function retains and utilizes this valuable feedback. Conversely, if a harmful (P3) reward is received, it is promptly sent back to the action function, effectively discarding it. This selective treatment of negative rewards involves binary choices, representing positive (P1) as '1' and

4

www.czasopisma.pan.pl   PAN   www.journals.pan.pl

Enhancing MPPT in Partially Shaded PV Modules: A Novel Approach using Adaptive Reinforcement Learning with Neural Network Architecture

negative (P3) as '0.' By disregarding the '0' value, the reward function output experiences a boost. In the context of MPPT, the reward function focuses on processing P1 values, characterized by their positive nature on the curves. The execution of the function, based on the input value of P_{maxp}, leads to the determination of a P2 value (ΔP_{maxp}) when nearing P_{maxp}, with P2 equating to 0. This P2 value becomes the conclusive result for the tracking process, embodying the GMPPT value. The output of the reward function encompasses optimized maximum current, voltage and current (ΔI_{maxp}, ΔV_{maxp} and ΔP_{maxp}), where the P2 value plays a pivotal role in the characteristic curves. Throughout NNA processing, the agent function undergoes refinement, contributing to heightened performance and precision. Equation 19 encapsulates the optimal reward function, underscoring the iterative nature of this process geared towards achieving the finest GMPPT results.

$$\text{Reward function} = \begin{cases} \text{Positive(P1), P>0} \\ \text{Zero(P2), \quad P=0} \\ \text{Negative(P3), P<0} \end{cases} \quad (19)$$

As shown in equation 20, this iterative process allows the agent to continuously refine its strategies, ultimately enhancing its decision-making capabilities over time.

$$\text{Objective function} = \Delta P_{maxp}, P2(\text{Reward}) \quad (20)$$

3.3. NNA training process

The NNA training processes represent a three processing layers [33]; there are two input layers, one single hidden layer, and one output layer. The input layer encompasses voltage and current values, while the output layer represents the optimized maximum power value. During the training process, a single hidden layer is typically equipped with N number of neurons. However, relying solely on a single hidden layer within the NNA training model may not suffice for effectively handling nonlinear data. To address the challenges posed by complex nonlinear data, NNA training models are employed. The purpose is to simplify the complexity associated with training such data. In this setup, the NNA receives and processes the finest reward and harmful reward value. In the NNA models, a feed-forward neural network (FFNN) is implemented to facilitate quick processing and generate effective outputs. Additionally, this approach aids in reducing the complexity encountered during the training of the data. Throughout the training process, the agent retains the finest reward as shown in equation 21, while the harmful reward is discarded, allowing for more effective learning.

The FFNN works under the process,

$$\text{FFNN} = \sum_{i=1}^{s} M \sum_{k=1}^{g} x_{(k,g)}, w_{(k,g)}, b_{(k,g)} \quad (21)$$

Where, M=1, while w and b represent the weight and bias value with the range of [1, 2,…, (k,g)] and x represents the PV modules' input parameters (V_{ocp}, I_{sch}, I_{maxp}, V_{maxp} and P_{maxp}) of the training process.

$$'\!\int' = S_{af}(p) \quad (22)$$

where '$\int$' represent the sigmoid activation function as shown in equation 22. The Sigmoid activation function is ($\int$): $S_{af} = \frac{1}{1+e^{-u}}$ where e = Euler's number.

A significant advantage of this approach is its ability to handle high-dimensional inputs, which is made possible by the absence of backward connections within the neural network architecture. The output generated through the trained feed-forward neural network (FFNN) is deemed accurate, characterized by minimal error values. Additionally, the use of the sigmoid activation function in the current training set contributes to achieving highly

effective output results, further enhancing the performance of the system.

Figure 4 illustrates the operational process of the ARL-NNA algorithm. The NNA training process involves two input layers, one hidden layer, and one output layer for each set of NNA. The two inputs represent the current and voltage values, which are then processed to produce an output using the iterative method. Furthermore, the hidden layer is equipped with 10 neurons for each set of NNA during the training process. The real-time characteristic curves data featuring roughly 5000 data points are divided into 70% (3500 data points) for training and 30% (1500 data points) for testing to ensure a robust evaluation of the system's performance. Then, the output layer represents the optimize power value (ΔP_{maxp}). Notably, the Sigmoid activation function and the Adam optimizer are employed in the NNAs training process. A total of 1000 epochs are utilized for both training and testing in the NNA process, contributing to the refinement of the algorithm.
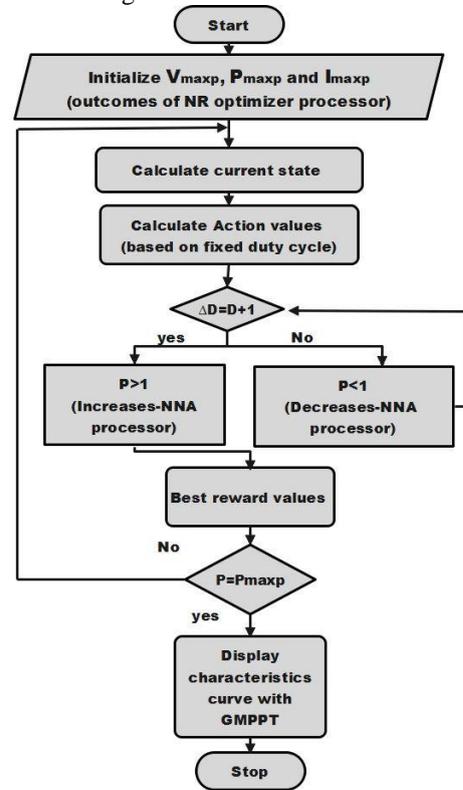

Fig. 4. Flowchart of ARL-NNA algorithm

The proposed algorithm assesses the performance of a PV module by considering several factors to demonstrate its effectiveness:

3.3.1. Percentage error for maximum peak power (e_{MPP})

The factor, as detailed in reference [34], assesses the percentage difference between maximum power values under partial shading conditions ($P_{mp(psp)}$) and datasheet values ($P_{mp(data)}$), relative to the maximum power under normal operating conditions ($P_{mp(noc)}$), expressed in equation 23.

$$e_{MPP} = \frac{P_{mp(data)} - P_{mp(psp)}}{P_{mp(noc)}} * 100 \quad (23)$$

3.3.2. Mismatching power loss (M_{pl})

The Mismatching Power Loss (M_{pl}), outlined by equation 24 and elaborated in [33], gauges the discrepancy between the sum of experimental powers under different partial shading

5

www.czasopisma.pan.pl   PAN   www.journals.pan.pl

Enhancing MPPT in Partially Shaded PV Modules: A Novel Approach using Adaptive Reinforcement Learning with Neural Network Architecture

patterns (P_{emp}) and the global maximum powers (P_{gmp}) observed during PV module operation, offering insights into efficiency losses during partial shading patterns.

$$M_{PL} = \frac{P_{emp} - P_{gmp}}{P_{emp}} \qquad (24)$$

3.3.3. Fill factor (FF)

The fill factor, according to equation 25 as described in [34], measures the ratio of the global maximum power generated by a PV module under partial shading patterns to the experimental power produced at the open-circuit voltage and short circuit-current.

$$Fill\ Factor = \frac{P_{gmp}}{V_{opc}I_{shC}} \qquad (25)$$

3.3.4. Root mean square error (RMSE)

The disparity between the partial shading patterns current and the normal operating condition current (I_{noc}) is signified by the root mean square error (RMSE) [33]. Equation 26 gives the mathematical description.

$$RMSE = \sqrt{\frac{\sum_{i=1}^{n}[(I_{maxp} - I_{noc})^2]}{I_{noc}}} * 100 \qquad (26)$$

4. RESULT AND ANALYSIS

Section 4 outlines a comprehensive procedure for handling accumulated experimental characteristic curve data from partial shading patterns, employing the innovative ARL-NNA algorithm. Rigorous experimentation and comparative analyses with existing algorithms validate the results, ensuring the robustness and reliability of the proposed algorithm through scrutiny of various error metrics and processing times. This systematic approach not only advances understanding of partial shading effects but also establishes the efficacy of the ARL-NNA algorithm in real-world applications.

4.1. Experimental data summary

Section 4.1, presents the input values representing partial shading patterns, which have been collected through experimental data obtained from our Power and Energy Management Laboratory. Due to partial shading, the output of PV module debilitates and the characteristics curve exhibit values in multiple peaks. The experimental setup of the PV module with partial shading patterns is shown in Fig. 5. In the present research work, 13 partial shading patterns are investigated. They are convened in the following patterns such as normal, centre, centre 20% shaded, diagonal, left bottom 30% shaded, top left shaded, random, bottom right shaded, right top 40% shaded, 4th row fully shaded, second column fully shaded, condition during and post rain as presented in Fig. 6a-6m.

The input parameters for the UEP, as specified in section 2, are experimentally collected using the SVL-0050P mono crystalline PV module type with specifications of I_{shc}=3.06A, V_{opc}=21.8V, I_{maxp}=2.87A, V_{maxp}=17.1V and P_{maxp}=50W.The PV module setup employs a voltmeter with a range of 0-200 V DC, an ammeter with a range of 0-20A DC, and a rheostat with a range of 0-200Ω and a maximum current of 5A. The IC3202B features 12-bit resolution and operates within a temperature range of -40° to 85°C. The digital display values are facilitated by IC 23741, with a capacitor model denoted as 508C2 (m) and a relay model specified as JQC-3FF-S-Z, supporting a maximum load of 250V/10A AC and 30V/10A DC, with a trigger current of 5mA and a working voltage of 5V. Additionally, the photo coupler (PC817C) features a collector-emitter output voltage of 35V, an emitter-collector output voltage of 6V, an input forward current of 50mA, an input power dissipation of 70mA, and a storage

temperature range of -55° to 25°C.
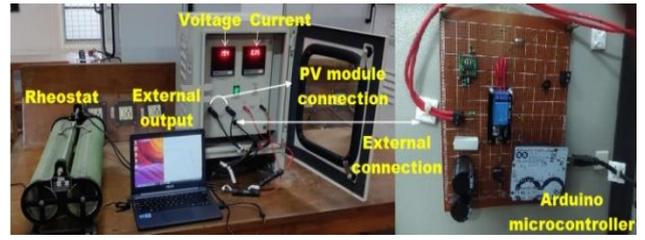
Fig. 5. Experimental setup of the PV module

Fig. 6(a). Pattern-I   **Fig. 6(b).** Pattern-II   **Fig. 6(c).** Pattern-III

Fig. 6(d). Pattern-IV   **Fig. 6(e).** Pattern-V   **Fig. 6(f).** Pattern-VI

Fig. 6(g). Pattern-VI   **Fig. 6(h).** Pattern-VIII   **Fig. 6(i).** Pattern-IX

Fig. 6(j). Pattern-X   **Fig. 6(k).** Pattern-XI   **Fig. 6(l).** Pattern-XII

Fig.6(m). Pattern-XIII

Fig. 6a-6m. Assorted types of partial shading patterns

Table 1 presents an overview of the experimentally collected data from the laboratory. Pattern I represents the reference case, which demonstrates the PV module's behavior under normal conditions without partial shading. In contrast, Patterns II to XI represent various basic partial shading patterns. Patterns XII and XIII, on the other hand, encompass scenarios during and after rainfall. The collection of partial shading patterns is further organized into various combinations. In each of these permutations, the values of the PV module parameters change due to the specific partial shading patterns applied.

The extension parameter values are obtained through experimental data and are subsequently employed in the Newton-Raphson method along with the product of I-V (current-voltage) and P-V (power-voltage) characteristic curves. The proposed ARL-NNA algorithm plays a vital role in refining the behavior of the PV module and extracting the optimal PV power output under the diverse experimental partial shading patterns. Finally, the trained model in the proposed algorithm produces an output that is displayed for further analysis and evaluation.

6

Enhancing MPPT in Partially Shaded PV Modules: A Novel Approach using Adaptive Reinforcement Learning with Neural Network Architecture

Table 1. Experimental input values of PV module

Pattern No.	Partial shading patterns	Experimental input parameters values				
		I_{shc} (A)	V_{opc} (V)	I_{maxp} (A)	V_{maxp} (V)	P_{maxp} (W)
I	Normal condition	1.86	19.9	1.71	14.8	25.3
II	Centre	0.35	19.3	0.26	17.4	4.56
III	Centre 20% shaded	0.87	20.1	0.74	17.5	13.0
IV	Diagonal	0.52	19.4	0.46	17.3	8.03
V	Left bottom 30% shaded	1.59	19.7	0.51	18.0	9.22
VI	Top left shaded	1.96	19.6	1.73	5.34	9.24
VII	Random	0.49	19.3	0.42	17.1	7.30
VIII	Bottom right shaded	1.55	19.6	1.36	6.45	8.78
IX	Right top 40% shaded	1.56	19.6	1.41	6.24	8.83
X	4th row fully shaded	0.44	19.7	0.38	17.9	6.89
XI	Second column fully shaded	1.53	19.5	1.40	6.32	8.85
XII	Rainy condition	0.30	19.8	0.27	15.5	4.34
XIII	Post-rain condition	0.59	20.5	0.54	16.6	9.12

4.2. Analysis of tracking process

The Power and Energy Management Lab at Thiagarajar College of Engineering, Madurai, is the focal point for experimental data collection on 13 diverse partial shading patterns. Utilizing IV-Swinger software for analysis and MATLAB 2019a for pattern execution, the study employs the existing and ARL-NNA algorithm for a meticulous tracking process to determine optimal operational points based on current vs. voltage and power vs. voltage characteristics. Results are compared with existing algorithms, and validation is performed using various error metrics. The gathered parameters are input into classical and soft computing algorithms, and both existing and proposed algorithms undergo a tracking process with a fixed duty cycle value, validated at different angular positions within characteristic curves. The identification of the Global Maximum Power Point Tracking (GMPPT) involves adjusting angular positions from positive (P1), zero (P2) and negative (P3), with P2 emerging as the GMPPT. Subsequent sections delve into the techniques employed for obtaining outputs under partial shading conditions using the existing and ARL-NNA algorithm, providing insights into the testing, training, and execution of the tracking process across both algorithmic approaches.

4.3. Appraisal of existing algorithms

In the comprehensive evaluation of algorithms targeting the identification of P2, as depicted in Fig. 3 as the Global Maximum Power Point Tracking (GMPPT), a cohesive approach was employed to evaluate various methodologies. The evaluated algorithms encompassed traditional techniques such as Perturb and Observe (P&O) and Incremental Conductance (InC), alongside more sophisticated approaches like Particle Swarm Optimization (PSO), Artificial Neural Network (ANN), Deep Neural Network (DNN), and Q-learning. The experimentation involved rigorous iterations and parameter tuning for each algorithm. P&O and InC were subjected to 1000 iterations with a fixed duty cycle (ΔD=0.01+weight), while PSO underwent a similar number of iterations with cognitive and social learning (c_l= 2, and c_s = 0.1) parameters and a weight range (w=1 to 0). Real-time characteristic curves were meticulously collected, totaling 5000 data points. For ANN and DNN, data allocation of 70% for training, and 30% testing was performed, with specific architecture details including 3 hidden layers, 100 neurons, and sigmoid activation functions. The Q-learning algorithm was characterized by a normalization constant (α=0.1), a discount factor (Ψ=0.9), and a set number of iterations. The outcomes of these evaluations, encompassing 13 different patterns, were summarized in Table 2, illustrating the optimized power values (ΔP_{maxp}(W)) while execution with different algorithms. This systematic analysis provides valuable insights into the performance and applicability of diverse algorithms for GMPPT, contributing to the advancement of power point tracking methodologies. The error analysis are evaluated based on difference between the actual power values (P_{maxp}(W)) and optimized power value (ΔP_{maxp}(W)) to estimate algorithms performance in accurately optimizing PV module output under different partial shading patterns.

4.4. Estimation of proposed ADL-NNA algorithm

In the investigation of the photovoltaic (PV) module's performance under diverse partial shading patterns, the proposed Adaptive Reinforcement Learning with Neural Network Architectures (ARL-NNA) is introduced as a key analytical tool. The empirical assessment, as delineated in Table 3, encompasses the execution of characteristic curve values using the innovative ARL-NNA. The resultant I-V and P-V characteristic curves are shown in Figs. 7(a)-7(z). Firstly, this evaluation is conducted under normal conditions (pattern-I), as illustrated in Figs. 7(a) and 7(b). The subsequent tracking process at various angles, represented by values P1, P2, and P3, unveils the algorithm's ability to pinpoint P2 as the Global Maximum Power Point Tracking (GMPPT). Then, the exploration of 12 additional partial shading patterns as shown in Figs. 7(c)-7(z) is executed. Pattern XII, as depicted in Figs. 7(c) and 7(d), is notably identified as particularly disruptive due to its susceptibility to unpredictable environmental changes, posing potential risks of overloading and equipment injury. In the context of mitigating the adverse effects of partial shading on both the PV module and interconnected electrical systems, the accurate estimation of PV module parameters, as detailed in Table 3, is a crucial aspect. These parameters are extracted and optimized using the proposed ADL-NNA algorithm, ensuring a comprehensive understanding and effective mitigation of partial shading effects on solar power systems.

The study underscores the importance of precise parameter estimation to navigate substantial challenges arising from partial shading scenarios. By offering comprehensive insights into the dynamic behavior of the PV module under diverse conditions, the research paves the way for a deeper understanding of how environmental changes influence performance and necessitates proactive measures to ensure the stability and reliability of the interconnected electrical systems. The integration of ARL-NNA as a novel algorithm contributes to the study's innovation, promising enhanced accuracy in tracking and mitigating the impact of partial shading on PV module performance.

Enhancing MPPT in Partially Shaded PV Modules: A Novel Approach using Adaptive Reinforcement Learning with Neural Network Architecture

Table 2. Calculated optimized power value (ΔP_{maxp}(W)) for different partial shading patterns using existing algorithms

Algorithm / Patterns	Without algorithm	Error (%)	P&O	Error (%)	InC	Error (%)	PSO	Error (%)	ANN	Error (%)	DNN	Error (%)	q-learning	Error (%)
Pattern-I	25.053	2.247	24.06	1.235	24.089	1.210	24.081	1.218	24.119	1.180	24.007	1.292	24.032	1.267
Pattern-II	4.246	0.313	4.345	0.214	4.359	0.206	4.343	0.216	4.313	0.245	4.313	0.246	4.312	0.247
Pattern-III	12.487	0.513	12.502	0.497	12.490	0.509	12.499	0.509	12.488	0.512	12.488	0.511	12.465	0.504
Pattern-IV	7.820	0.209	7.802	0.227	7.802	0.227	7.802	0.227	7.802	0.227	7.802	0.227	7.802	0.227
Pattern-V	8.279	0.940	8.194	1.025	8.388	0.831	8.485	0.734	8.487	0.732	8.379	0.840	8.384	0.835
Pattern-VI	8.231	1.008	8.171	1.069	8.205	1.034	8.680	0.559	8.356	0.883	8.757	0.482	8.471	0.768
Pattern-VII	6.462	0.838	6.448	0.851	6.233	1.066	6.205	1.094	6.215	1.084	6.232	1.067	6.236	1.063
Pattern-VIII	7.970	0.809	8.134	0.645	8.149	0.630	7.927	0.852	8.326	0.454	8.320	0.459	7.932	0.847
Pattern-IX	8.526	0.303	8.508	0.321	8.527	0.303	8.574	0.255	8.565	0.264	8.560	0.269	8.572	0.258
Pattern-X	6.610	0.280	6.522	0.368	6.648	0.241	6.649	0.246	6.639	0.250	6.622	0.267	6.626	0.263
Pattern-XI	8.687	0.162	8.602	0.247	8.600	0.249	8.609	0.240	8.590	0.260	8.688	0.161	8.600	0.249
Pattern-XII	4.119	0.220	4.104	0.235	3.993	0.347	4.105	0.234	3.954	0.385	3.996	0.343	3.902	0.437
Pattern-XIII	8.866	0.253	8.855	0.264	8.861	0.258	8.817	0.302	8.8025	0.317	8.846	0.273	8.851	0.268

Table 3. Estimation of PV module parameters under assorted partial shading patterns for the proposed ARL-NNA algorithm

S. No.	Parameters/ patterns	Extracted parameters					Characteristic curve values					Error (%) (P_{maxp}-ΔP_{maxp})
		A	I_o (A)	I_{ph} (A)	R_{se} (Ω)	R_{ph} (Ω)	ΔI_{maxp} (A)	ΔV_{maxp} (V)	ΔP_{maxp} (W)	I_{shc} (A)	V_{opc} (V)	
1.	Pattern-I	1.00	$6.731e^{-08}$	1.866	0.037	506.207	1.706	14.785	25.219	1.820	17.383	80.1×10^{-3}
2.	Pattern-II	2.30	$4.168e^{-06}$	0.344	5.236	250.795	0.259	17.379	4.515	0.288	18.945	44.6×10^{-3}
3.	Pattern-III	1.37	$1.492e^{-08}$	0.871	0.101	303.157	0.739	17.419	12.563	0.863	18.608	437.0×10^{-3}
4.	Pattern-IV	1.28	$1.027e^{-09}$	0.503	0.415	701.855	0.458	17.245	7.908	0.518	20.998	121.1×10^{-3}
5.	Pattern-V	1.44	$2.237e^{-08}$	0.623	0.101	356.702	0.484	17.975	8.700	0.653	20.216	519.3×10^{-3}
6.	Pattern-VI	1.19	$4.134e^{-09}$	2.639	7.326	21.365	1.703	5.254	8.956	1.958	18.765	284.0×10^{-3}
7.	Pattern-VII	1.04	$1.063e^{-10}$	0.488	1.218	1753.083	0.393	17.025	6.562	0.487	18.998	738.0×10^{-3}
8.	Pattern-VIII	1.13	$6.272e^{-08}$	1.670	5.378	67.846	1.343	6.355	8.539	1.538	15.768	240.7×10^{-3}
9.	Pattern-IX	1.13	$6.917e^{-09}$	1.745	6.904	58.252	1.407	6.201	8.590	1.559	17.787	239.1×10^{-3}
10.	Pattern-X	2.48	$1.303e^{-05}$	0.421	4.772	177.725	0.379	18.768	6.762	0.439	18.803	127.8×10^{-3}
11.	Pattern-XI	1.09	$1.052e^{-09}$	1.741	9.031	65.989	1.383	6.319	8.739	1.527	20.659	110.1×10^{-3}
12.	Pattern-XII	1.04	$2.333e^{-10}$	0.308	1.544	2086.036	0.268	15.499	4.155	0.299	17.958	184.5×10^{-3}
13.	Pattern-XIII	1.00	$1.971e^{-09}$	0.592	0.674	734.887	0.539	16.576	8.846	0.589	19.558	273.9×10^{-3}
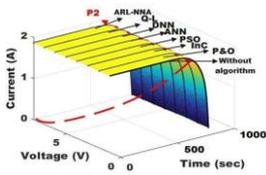
Fig. 7(a).
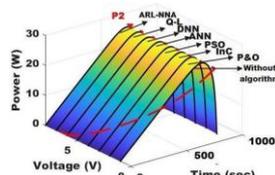
Fig. 7(b).
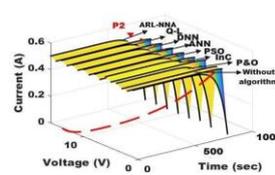
Fig. 7(g).
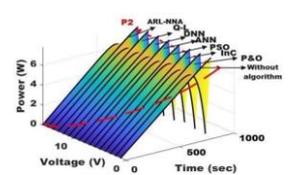
Fig. 7(h).
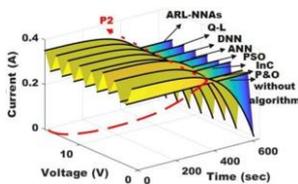
Fig. 7(c).
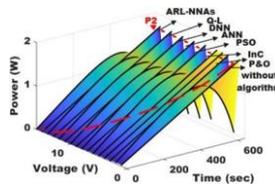
Fig. 7(d).
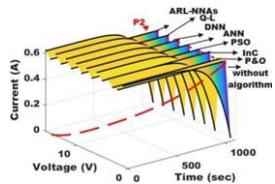
Fig. 7(i).
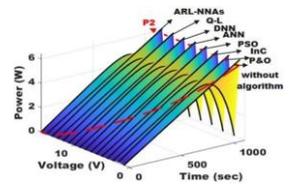
Fig. 7(j).
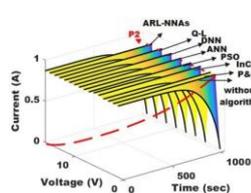
Fig. 7(e).
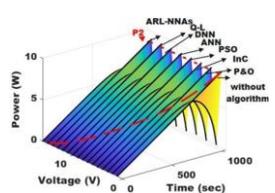
Fig. 7(f).
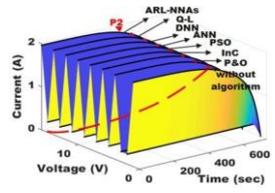
Fig. 7(k).
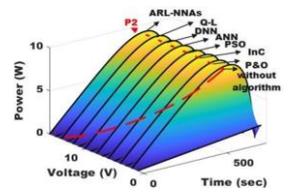
Fig. 7(l).

www.czasopisma.pan.pl PAN www.journals.pan.pl

Enhancing MPPT in Partially Shaded PV Modules: A Novel Approach using Adaptive Reinforcement Learning with Neural Network Architecture
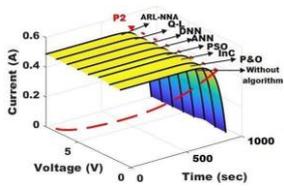
Fig. 7(m).
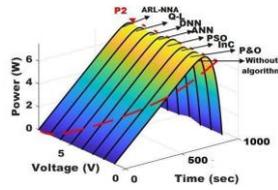
Fig. 7(n).
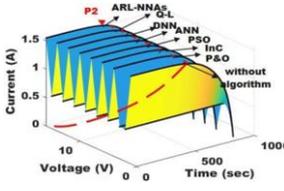
Fig. 7(o).
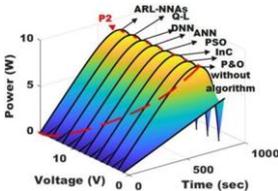
Fig. 7(p).
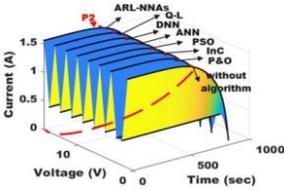
Fig. 7(q).
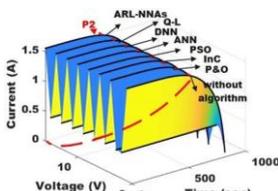
Fig. 7(r).
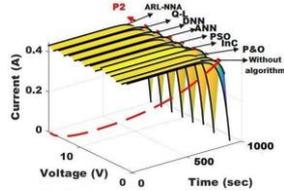
Fig. 7(s).
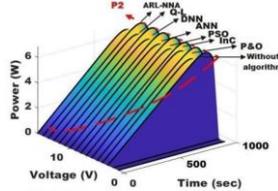
Fig. 7(t).
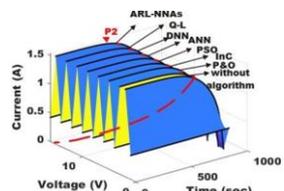
Fig. 7(u).
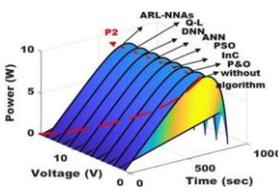
Fig. 7(v).
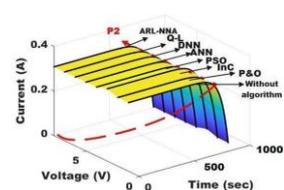
Fig. 7(w).
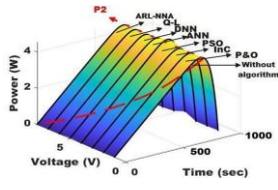
Fig. 7(x).
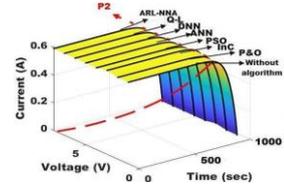
Fig. 7(y).
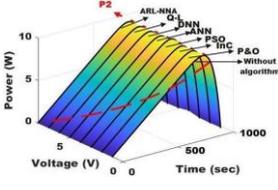
Fig. 7(z).

Fig. 7(a)-7(z). Characteristics curves (IV & PV) of PV module for different patterns

4.5. Discussion of outcomes

The experimental and simulated results for the thirteen partial shading patterns present estimated outcomes, incorporating diverse error types such as Percentage Error for Maximum Peak Power (e_{mpp}), Mismatch Power Loss (M_{pl}), Fill Factor (FF), Root Mean Square Error (RMSE), and processing time. Both existing algorithms and the proposed algorithm undergo calculation of these error metrics, enabling a thorough and comprehensive comparison across different performance criteria.

4.5.1. Evaluation of different factors

Figures 8-11 showcase 3D bar graphs representing different miscalculation factors and the results are further validated with diverse error metric values. The study compared the performance of various optimization algorithms, including without algorithm, P&O, InC, PSO, ANN, DNN, q-learning, and ARL-NNA, across thirteen partial shading patterns (P-I to P-XIII), evaluating factors like percentage error of maximum peak power (e_{mpp}), mismatching power loss (M_{pl}), fill factor, and root mean square error (RMSE) to assess their effectiveness in enhancing solar panel efficiency under different shading conditions. Notably, the ARL-NNA algorithm consistently demonstrates lower error values across all thirteen partial shading patterns. This substantiates the exceptional performance of the proposed ARL-NNA algorithm, emphasizing its superiority compared to the mentioned existing algorithms in handling and minimizing errors.
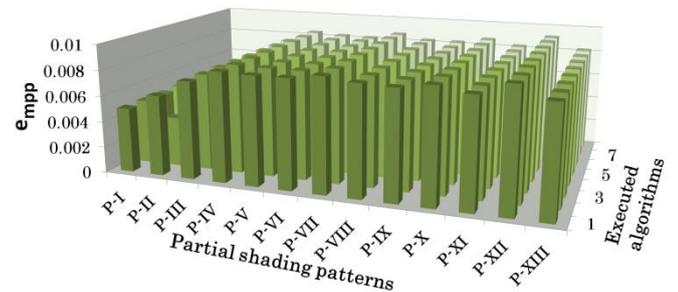

Fig. 8. e_{mpp} of various algorithms
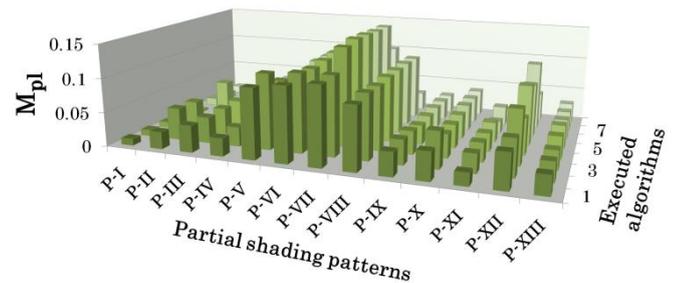
Fig. 9. M_{pl} of various algorithms
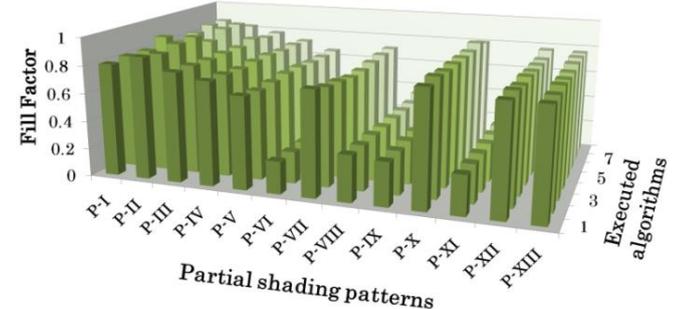
Fig. 10. FF of various algorithms

9

www.czasopisma.pan.pl PAN www.journals.pan.pl

Enhancing MPPT in Partially Shaded PV Modules: A Novel Approach using Adaptive Reinforcement Learning with Neural Network Architecture
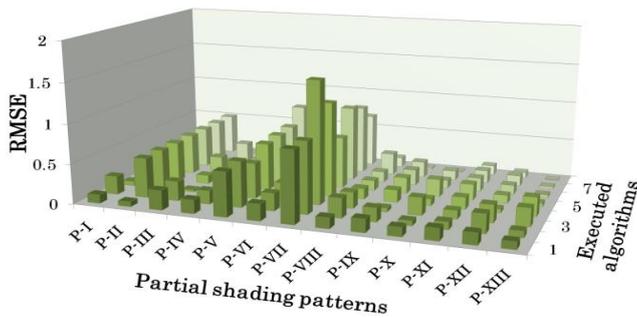

Fig.11. RMSE of various algorithms

4.5.2. Estimation of processing time

The assessment of proposed algorithms with varying processing times, as depicted in Fig. 12, is incorporated in MATLAB 2019a in Intel core I3 processor. It is evident that fundamental, analytical, and classical algorithms exhibit slightly extended durations when compared to alternative methods. Notably, Bio-Inspired and Soft Computing algorithms demonstrate marginally shorter processing times. However, the general process executed for all patterns, in the absence of a specific algorithm, remains consistent at a duration ranging from 1.23 to 1.58 seconds. Contrastingly, existing algorithms such as P&O, InC, PSO, ANN, DNN, and q-learning operate within a narrower time frame, spanning from 1.03 to 1.55 seconds.

Remarkably, the ARL-NNA algorithm emerges as a standout performer in terms of rapid execution and precise tracking of maximum values. It remarkably accomplishes the tracking process for all patterns within an exceptionally brief timeframe, ranging from a mere 0.32 to 0.52 seconds.
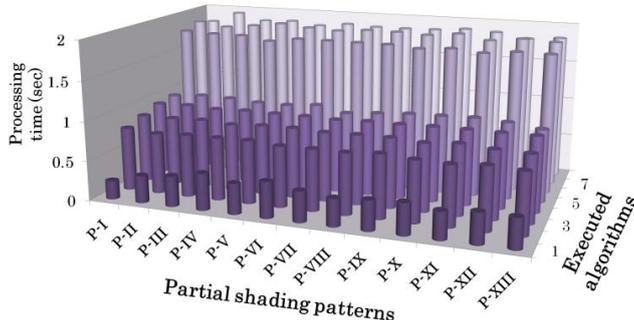

Fig. 12. Processing time of various algorithms

Furthermore, this algorithm generates fewer error values compared to existing methodologies, underscoring its efficiency in handling maximum unknown electrical parameters. The swift and accurate performance of the ARL-NNA algorithm positions it as a promising contender for optimizing power point tracking processes, showcasing its potential to outperform traditional and contemporary algorithms in this domain.

4.5.3. Comparison of different MPPT algorithms

The comparison of Maximum Power Point Tracking (MPPT) algorithms for solar power as depicted in Fig. 13, offers valuable insights to their respective performances. Fig. 13 utilizes a scoring system ranging from 0 to 10, to track the least and best-performing parameters. The evaluation is based on the analysis of existing literature reviews, the study of various algorithms as put forth in Table 4, and the numerical computing in MATLAB simulations.

Among the algorithms assessed, the ARL-NNA algorithm emerged as the top performer, gathering the highest average score. This highlights its efficiency in optimizing power generation in solar systems. Following closely behind are established methods

like P&O, InC, PSO, ANN, DNN, and Q-l algorithms, showcasing their adaptability and effectiveness in navigating the dynamic operational environments of PV module power under partial shading conditions. The study underscores the pivotal role of artificial intelligence (AI) technics in striking a balance between algorithm complexities and achieving desirable MPPT performance. By leveraging classical, Bio-inspired and soft computing algorithms the study demonstrates promise in enhancing the efficiency and reliability of solar energy systems, paving way for sustainable energy solutions.
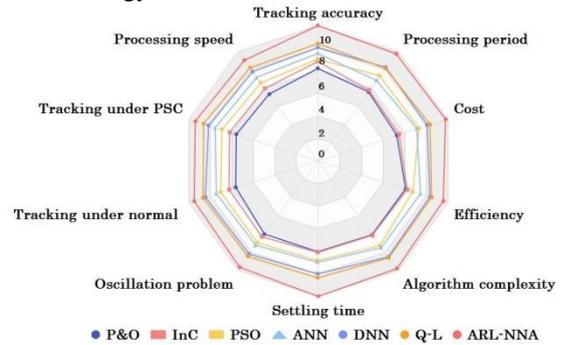

Fig. 13. Performance estimation of AI-based MPPT algorithms

The comparative analysis as shown in Table 4 delves into a variety of methods for identifying the MPPT in PV modules [35]. It encompasses conventional techniques like P&O and InC, which are valued for their simplicity and reliability but may struggle to adapt to changing conditions. In contrast, modern approaches such as Bio-inspired (BI) and artificial intelligence algorithms like PSO, ANN, DNN and q-learning offer increased flexibility and precision, especially in scenarios involving partial shading and unpredictable environmental conditions. Additionally, the proposed adaptive reinforcement learning with neural network architecture (ADL-NNA) algorithm within the realm of ML further enhances accuracy, albeit with higher computational difficulty and data needs.

The selection of a method depends on the precise application, by simpler techniques remaining effective in less complex situations, while superior machine learning approach, including reinforcement learning algorithms, become increasingly essential for PV systems optimizing in demanding actual world circumstances. The comprehensive investigation of all partial shading patterns follows a consistent procedure to observe the tracking process at zero angles.

During the testing and training of the ARL-NNA algorithm, the optimal reward function value for maximum power is established through multiple iterations to enhance precision. The outcomes of the executed algorithms are rigorously validated using various error metrics. Consequently, it can be concluded that the ARL-NNA algorithm indeed exhibits minimal errors, and the processing time required is significantly shorter, measured in fractions of a second, compared to any other algorithms mentioned in the study. This study also significantly impacts various realms of electrical engineering, introducing pioneering methods in Power Systems through a novel PV module using MPPT, potentially transforming solar energy integration into power grids.

10

Enhancing MPPT in Partially Shaded PV Modules: A Novel Approach using Adaptive Reinforcement Learning with Neural Network Architecture

Table 4. Comparing existing and proposed MPPT algorithms

Index	P&O	InC	PSO	ANN	DNN	q-learning	ARL-NNA
Tracking speed	Below	Below	Sensible	Speedy	Below	Speedy	Speedy
Tracking accuracy	Sensible	Sensible	Improved	Speedy	Weak	Speedy	Speedy
Processing speed	Elevated	Elevated	More	More	More	Speedy	Speedy
Tracking under PSC	Deprived	Deprived	Sensible	Sensible	Slow	Improved	Speedy
Tracking under normal condition	Sensible	Sensible	Sensible	Sensible	Sensible	Sensible	Improved
Oscillation problem	Certainly	Certainly	No	No	None	No	No
Tracking MPP	Low	Low	Elevated	Sensible	Weak	Speedy	Speedy
Complexity	Certainly	Certainly	Below	Certainly	Indeed	No	No
Input parameters	Voltage and Current	Voltage and current	Voltage and current	Voltage and current	Voltage and current	Voltage and current	Voltage and current
Processing tuning	Sensible	Sensible	Sensible	More	Below	More	More
Efficiency	Below	Below	Improved	More	Below	More	More
Processing period	Elevated	Elevated	Sensible	Below	Sensible	Low	Low
Cost	Elevated	Elevated	Elevated	Sensible	Elevated	Sensible	Sensible
Algorithm complexity	Certainly	Certainly	Sensible	Sensible	Indeed	Improved	Improved
Advantages	Simplicity	Overcome the oscillation problem	Global search effective	Below steady-state oscillation	Straight process	Efficient for global tracking	Efficient for tracking
Disadvantage	Oscillation problem	Increases of cost	Elevated-dimensional space	Cost elevated	Weak performance for non-linear data	More training data	Cost elevated
Applications	Grid	Grid	Grid and solar vehicles	On and off grid, solar vehicles	Microgrid	On and off grid, solar vehicles	On and off grid, solar vehicles

Power Electronics benefits from the advancement in Maximum Power Point Tracking techniques enhancing the efficiency of the power conversion systems. Solid state Electronics and Industrial Electronics gain insights into improving the performance of large-scale photovoltaic installations. The cross-disciplinary impact extends to Modern Information and Energy Technologies, where the integration of machine learning contributes to smarter and more adaptive energy systems, aligning with the evolving landscape of digitization and sustainability. Furthermore, the proposed approach utilizing the ARL-NNA algorithm consistently demonstrates superior performance compared to the aforementioned algorithms discussed in the study, even in the face of significant weather changes, steady-state conditions, oscillations due to fluctuated inputs, and the need to meet energy demands.

5. CONCLUSION

Solar energy is inevitable today and in future. To minimize the power loss in the solar energy conversion system, accurate Maximum Power Point Tracking of PV modules is essential for optimizing their performance under varying partial shading conditions and diverse climatic scenarios. In this study, we exposed the PV module to 13 different partial shading patterns using real-time experimental data to investigate the MPPT process. For accurate and speedy measurement of real time data of the PV module, we introduced a novel algorithm known as Adaptive Reinforcement Learning with Neural Network Architectures (ARL-NNA). This algorithm demonstrated the remarkable capability to modernize the MPPT process, to track the maximum power point along with characteristic curves within a fraction of second. Our study unequivocally concludes that the proposed ARL-NNA machine learning algorithm is highly

suitable for conducting the tracking process with fewer errors compared to other algorithms. Moreover, our research establishes that the proposed algorithm represents a viable means of swiftly tracking maximum power points. This research underscores the potential of machine learning and adaptive algorithms in advancing renewable energy technologies and beyond, emphasizing their role in shaping a more sustainable and efficient future. Looking ahead, the ARL-NNA algorithm presents a transformative solution that extends beyond photovoltaic systems. It opens up a multitude of possibilities for innovation and efficiency enhancement across various domains, including environmental forecasting, crop management optimization, energy efficiency enhancement, healthcare intervention support, and building energy use optimization.

REFERENCES

[1] "Solar PV," 2023. [Online]. Available: https://www.iea.org/energy-system/renewables/solar-pv/ (Accessed 2023-07-13).

[2] "Solar power by country," Wikipedia. [Online]. Available: https://en.wikipedia.org/wiki/Solar_power_by_country/ (Accessed 2023-02-15).

[3] "List of countries received snowfall," Academickids. [Online]. Available: https://academickids.com/encyclopedia/index.php/List_of_countries_receiving_snowfall/ (Accessed 2023-02-15).

[4] "Average precipitation by country," Trading Economics. [Online]. Available: https://tradingeconomics.com/country-list/precipitation/

Enhancing MPPT in Partially Shaded PV Modules: A Novel Approach using Adaptive Reinforcement Learning with Neural Network Architecture

(Accessed 2023-02-15).

[5] "List of cities by sunshine duration," Wikipedia. [Online]. Available: https://en.wikipedia.org/wiki/ List_of_cities_by_ sunshine_duration/ (Accessed 2023-02-15).

[6] S. Kinuthia, "The cloudiest city in the world," 2019. [Online]. Available: https://www.worldatlas.com/articles/cities-who-receive-the-least-sunshine.html/ (Accessed 2023-05-12).

[7] P. Srivastava, "In Pictures: The wettest places on earth!," 2022. [Online]. Available: https://timesofindia.indiatimes.com /travel/destinations /in-pictures-the-wettest-places- onearth/ photostory/ 92878425.cms? picid=92878621/ (Accessed 2023-01-05).

[8] J. Nobel, "The World's Snowiest Place is Starting to Melt," 2017. [Online]. Available: https://www.nationalgeographic.com /science /article/ worlds-snowiest-place-northwestern-japan-melting-climate-change?loggedin=true&rnd=1692861915026/ (Accessed 2023-03-13).

[9] B. Zbigniew, A. Krzysztof, K. Malgorzata, M. Janusz, W. Jacek and R. Antoni, "Review of photo detectors characterization methods," *Bulletin of the Polish Academy of Sciences. Technical Sciences*, vol. 70, no. 2, pp. 1-26, 2022. doi: 10.24425/bpasts.2022.140534

[10] M. Uoya and H. Koizumi, "A calculation method of photovoltaic array's operating point for MPPT evaluation based on one-dimensional Newton-Raphson method," *IEEE Trans. Ind. Appl*, vol. 51, no. 1, pp. 567–575, 2015. doi: 10.1109/TIA.2014.2326083

[11] A. Chatterjee, A. Keyhani, and D. Kapoor, "Identification of photovoltaic source models," *IEEE Trans. Energy Convers.*, vol. 24, no. 3, pp. 883–889, 2011. doi: 10.1109/TEC.2011.2159268

[12] W. Marańda and M. Piotrowicz, "Efficiency of maximum power point tracking in photovoltaic system under variable solar irradiance," *Bulletin of the Polish Academy of Sciences. Technical Sciences,* vol. 4, no. 4, pp. 713-721, 2014. doi: 10.2478/bpasts-2014-0077

[13] T. Sutikno, A. C. Subrata, G. Pau, A. Jusoh and K. IshaQue, "Maximum power point tracking techniques for low-cost solar photovoltaic applications–Part I: constant parameters and trial-and-error," *Archives of Electrical Engineering,* vol. 72, no. 1, pp. 125-145, 2023. doi: 10.24425/aee.2023.145410

[14] K. Y. Yap, C. R. Sarimuthu and J. M. Y. Lim, "Artificial Intelligence Based MPPT Techniques for Solar Power System: A review," *Journal of Modern Power Systems and Clean Energy*, vol. 8, no. 6, pp. 1043- 1059, 2020. doi: 10.35833/MPCE.2020.000159

[15] J. Ahmed and Z. Salam, "An enhanced adaptive P&O MPPT for fast and efficient tracking under varying environmental conditions," *IEEE Trans Sustain. Energy*, vol. 9, no. 3, pp. 1487–1496, 2018. doi: 10.1109/TSTE.2018.2791968

[16] A. Ilyas, M. Ayyub, M. R. Khan, A. Jain and M. A. Husain, "Realisation of incremental conductance the MPPT algorithm for a photovoltaic system," *Int. J. Ambient Energy*, vol. 39, no. 8, pp. 873-884, 2018. doi: https://doi.org/10.1080/01430750.2017.1354322

[17] A. M. Eltamaly, M. S. Al-Saud, A. G. Abokhalil and H. M. H. Farh, "Simulation and experimental validation of fast adaptive particle swarm optimization strategy for photovoltaic global peak tracker under dynamic partial shading," *Renewable and Sustainable Energy Reviews*, vol. 124, pp. 1-14, 2020. doi: https://doi.org/10.1016/j.rser.2020.109719

[18] D. Yousri, T. S. Babu, D. Allam, V. K. Ramachandaramurthy and M. B. Etiba, "A novel chaotic power pollination algorithm for global maximum power point tracking for photovoltaic system under partial shading conditions," *IEEE Access*, vol. 7, pp. 121432-121445, 2019. doi: 10.1109/ACCESS.2019.2937600

[19] L. Shang, W. Zhu, P. Li and H. Guo, "Maximum power point tracking of PV system under partial shading conditions through flower pollination algorithm," *Protection and Control of Modern Power Systems*, vol. 3, no. 4, pp. 1–7, 2018. doi: https://doi.org/10.1186/s41601-018-0111-3

[20] H. Wang, W. Wang, X. Zhou, J. Zhao, Y. Wang, S. Xiao and M. Xu, "Artificial bee colony algorithm based on knowledge fusion," *Complex & Intelligent Systems*, vol. 7, pp. 1139–1152, 2021. doi: https://doi.org/10.1007/s40747-020-00171-2

[21] L. Knypiński, "A novel hybrid cuckoo search algorithm for optimization of a line-start PM synchronous motor," *Bulletin of the Polish Academy of Sciences. Technical Sciences,* vol. 71, no. 1, pp. 1-8, 2023. doi:10.24425/bpasts.2023.144586

[22] G. K. J. Samuel, M. S. S. Sundari, R. Bhavani and A. J. Gnanamalar, "An efficient microgrid model based on Markov fuzzy demand-side management," *Bulletin of the Polish Academy of Sciences. Technical Sciences*, vol. 71, no. 3, pp. 1-8, 2023. doi: 10.24425/bpasts.2023

[23] T. Sun and C. Liu, "Fuzzy comprehensive model of manufacturing industry transfer risk based on economic big data analysis," *Bulletin of the Polish Academy of Sciences. Technical Sciences*, vol. 70, no. 2, pp. 1-8, 2022. doi: 10.24425/bpasts.2021.139959

[24] X. Tang, H. Li, J. Zhang, Z. Tang, H. Wang and C. Cal, "Anonymous traffic classification based on three-dimensional Markov image and deep learning," *Bulletin of the Polish Academy of Sciences. Technical Sciences*, vol. 71, no. 4, pp. 1-12, 2023. doi: 10.24425/bpasts.2023.145676

[25] M. Leelavathi and V. S. Kumar, "Deep neural network algorithm for MPPT control of double diode equation based PHV module," *Materials Today: Proceeding*, vol. 62, no. 7, pp. 4764–4771, 2022. doi: https://doi.org/10.1016/j.matpr.2022.03.340

[26] R. S. Sutton and A. G. Barto, *Reinforcement learning: An introduction*. England: MIT, 2018.

[27] X. Zhang, C. Li, Z. Li, X. Yin, B. Yang, L. Gan and T. Yu, "Optimal mileage-based PHV array reconfiguration using swarm reinforcement learning," *Energy Conversion Management*, vol. 232, p. 113892, 2021. doi: https://doi.org/10.1016/j.enconman.2021.113892

[28] L. Avila, M. De Paula, T. Maximiliano and I. Carlucho, "Deep reinforcement learning approach for MPPT control of partially shaded PHV systems in Smart Grids," *Applied Soft Computing*, vol. 97, Part B, p. 106711, 2020. doi: https://doi.org/10.1016/j.asoc.2020.106711

[29] R.C. Hsu, C. T. Liu, W. Y. Chen, H.I. Hsieh and H. L. Wang, "A Reinforcement Learning-Based Maximum Power Point Tracking Method for Photovoltaic Array," *International Journal of Photo energy*, vol. 2015, pp. 1-12, 2015. doi: https://doi.org/10.1155/2015/496401

[30] J. Sirignano and K. Spiliopoulos, "Asymptotics of reinforcement learning with neural networks," *Stochastic Systems*, vol. 12, no. 1, pp. 2–29, 2021. doi: https://doi.org/10.48550/arXiv.1911.07304

[31] A.K. Abdulrazzaq, G. Bognár and B Plesz, "Evaluation of different methods for solar cells/modules parameters extraction," *Solar Energy*, vol. 196, pp. 183–195, 2020. doi: https://doi.org/10.1016/j.solener.2019.12.010

[32] X. H. Nguyen and M. P. Nguyen, "Mathematical modeling of photovoltaic cell/module/arrays with tags in Matlab/Simulink," *Environmental Systems Research*, vol. 4, no. 24, pp. 1–13, 2015. doi: 10.1186/s40068-015-0047-9

[33] T. H. Le, L. Dai, H. Jang, and S. Shin, "Robust Process Parameter Design Methodology: A New Estimation Approach by Using Feed-Forward Neural Network Structures and Machine Learning Algorithms," *Applied Sciences*, vol. 12, no. 6, pp. 1-12, 2022. doi: https://doi.org/10.3390/app12062904

[34] E. A. Silva, F. Bradaschia and M.C. Cavalcanti, and A. J. Nascimento, "Parameter estimation method to improve the accuracy of photovoltaic electrical model," *IEEE Journal of Photovoltaics*, vol 6, no. 1, pp. 278-285, 2016. doi: 10.1109/JPHOTOV.2015.2483369

[35] M. Leelavathi, V. S. Kumar and B. Devi, "Maximizing Solar Energy Output: A Comparative Analysis of MPPT Strategies for Partially Shaded PV Systems," in *2023 International Conference on Energy, Materials and Communication Engineering (ICEMCE)*. India, 2023, pp. 1-7. doi: 10.1109/ICEMCE57940.2023.10434173